

# Applications of Electron Beam-induced Current at p-n Junction in InSb Devices

Xiangle Sun<sup>1,4</sup>, Haichuan Yin<sup>1,\*</sup>, Xuegong Yu<sup>2</sup>, Qian Sun<sup>3</sup>, Xuqian Bai<sup>1</sup>

<sup>1</sup>Yunnan Light and Textile Vocational College, Kunming, China

<sup>2</sup>State Key Lab. of Si Materials, Zhejiang University, Hangzhou, China

<sup>3</sup>Yunnan University of Business Management, Kunming, China

<sup>4</sup>Special Device Cent, Kunming Institute of Physics, Kunming, China

## Email address:

13888778378@139.com (Xiangle Sun), 13987643041@139.com (Haichuan Yin)

\*Corresponding author

## To cite this article:

Xiangle Sun, Haichuan Yin, Xuegong Yu, Qian Sun, Xuqian Bai. Applications of Electron Beam-induced Current at p-n Junction in InSb Devices. *American Journal of Modern Physics*. Vol. 11, No. 3, 2022, pp. 52-59. doi: 10.11648/j.ajmp.20221103.11

**Received:** January 28, 2022; **Accepted:** February 16, 2022; **Published:** May 7, 2022

---

**Abstract:** Being able to visually “see” a p-n junction in a semiconductor is advantageous to the design and fabrication of semiconductor devices. Electron beam-induced current (EBIC) was employed in this study to observe the p-n junction in InSb devices, and both Schottky and p-n junctions were observed through EBIC signal distribution. The temperature dependence of Cr-InSb (chromium-indium antimonide) Schottky junction was discovered unexpectedly. When Schottky junction’s temperature decrease, Schottky junction itself will have a new space charge region. This new space charge region is out of Schottky junction itself. Both the new space charge region and Schottky junction’s space charge region have same character. The new space charge region will enlarge with temperature decrease. This new space charge region is called Schottky response zone. For a InSb device which uses Cr as the Ohmic contact material, the Schottky junction was formed at the Cr-InSb interface. The Schottky response zone extends to 47 $\mu$ m at 80K. The space charge region of the p-n junction fabricated using ion-beam implantation in the InSb device has an asymmetrical spatial distribution. The aforementioned region on the n-type side is thinner and has larger charge density than that on the p-type side. As one of the most useful analytical methods, EBIC offers the advantage of a microscopic and perspective view for the observation and analysis of semiconductor devices without damaging the devices themselves.

**Keywords:** Electron Beam-induced Current, Schottky Junction, p-n Junction, InSb Device

---

## 1. Introduction

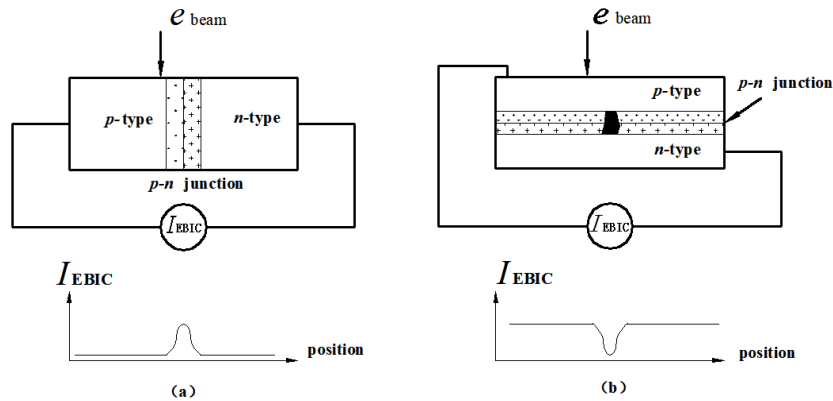
Precisely determining the position of microstructures (such as p-n junction, defects, etc.) in the semiconductor devices is important to the design and fabrication technique of the semiconductor devices manufacturing technology. In a circuit interconnection process, for example, an Ohm hole is needed to be fabricated in the semiconductor through ion etching and metal film depositing. The Ohm hole cannot be etched too deep and too shallow. Too deep hole will make the Ohm hole across the p-n junction and cause the short circuit while too shallow hole will cause power dissipation increase. If the position of the p-n junction can be determined precisely, both problems of short circuit and power dissipation increase will be settled down.

When an electron beam strikes into the semiconductor sample, a lot of extra removable nonequilibrium carriers (electron hole pair) can be created. If a self-built electric field (p-n junction or Schottky junction) exists in the semiconductor or an extra electric field (external bias) is applied to the semiconductor, the extra carriers will be collected and form current signal. This current signal is electron beam-induced current (EBIC). By scanning the semiconductor sample surface with the electron beam and collecting the EBIC, the EBIC image of the microstructures (p-n junction, defects, etc.) in the semiconductor devices can be displayed [1].

EBIC can be used to measure the diffusion length of the minority carrier in the semiconductor material [2-4], the lifetime of the minority carrier [5, 6], the width of the

depletion layer [7, 8], and the surface recombination velocity of semiconductor material [9]. Schematic of EBIC at p-n junction is shown in Figure 1. In Figure 1(a), the electron beam is parallel to the p-n junction. While the electron beam scanning through the p-n junction, it stimulates electron hole pairs in the depletion layer. These electron hole pairs are collected by the self-built field, forming the EBIC signal. While the electron beam scanning other area, the extra electron hole pairs stimulated by the electron beam are

recombined with majority carriers. They do not contribute anything to the EBIC. In this way, the width of a p-n junction can be observed; In Figure 1(b), the electron beam is perpendicular to the p-n junction. When the electron beam scans on the surface of the sample, the area with good p-n junction beneath the surface will show bright EBIC image, while the area with defects or the area with no space-charge region will show dark EBIC image. In this way, the position of p-n junction can be precisely determined.



(a) Electron beam is parallel to the p-n junction (b) Electron beam is perpendicular to the p-n junction

Figure 1. Schematic of EBIC at p-n junction.

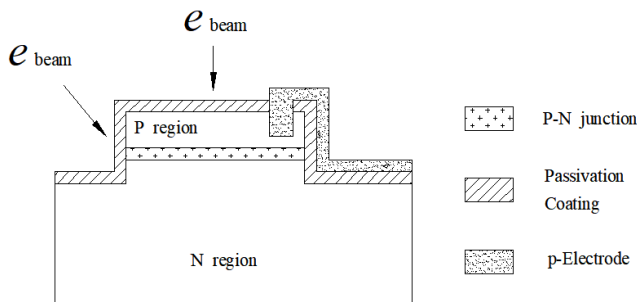


Figure 2. Preparation of the sample.

## 2. Sample Preparation

A slice of InSb<111> wafer with approximately 600 $\mu\text{m}$  thickness was employed for the substrate of the sample. After polishing process, a SiO<sub>2</sub> film of approximately 100nm thickness was deposited on the polished side of the substrate with PECVD (plasma enhanced chemical vapor deposition). A p-n junction was implanted under the SiO<sub>2</sub> film of the sample by Be<sup>+</sup> ion implantation. After a series of annealing, etching (of the 100nm thickness SiO<sub>2</sub> film), and photoetching, a mesa structure (photosensitive area) with p-n junction in it was formed. In order to make it easy for the EBIC measurement, the p region was thinned by etching. A SiO<sub>2</sub> passivation film about 700nm thickness was deposited by PECVD. Then the Ohm hole, the electrodes were photoetched and etched (ion beam etching) and a Cr+Au compound film was deposited by magnetron sputtering, the Cr film (about 100nm thickness) for Ohm hole, the Au film (about 500nm thickness) for electrodes. See Figure 2.

In order to easy SEM (scanning electron microscope) observation, a part of the Au film was etched off. The sample's SEM Images are Figure 3. Figure 3(a) is the SEM image as the electron beam is perpendicular to the sample's surface. The Y-shape area is the p electrode of the sample. Three O-shape areas are in the image. The biggest O-shape area with 240 $\mu\text{m}$  in diameter is the mesa structure with p-n junction in it. The second large O-shape area has 160 $\mu\text{m}$  in diameter. The smallest O-shape area with 66 $\mu\text{m}$  in diameter is the Ohm hole which connects p region of the sample and p electrode. See Figure 2. Figure 3(b) is sample's lateral profile SEM image. There is an angle of 162° between electron beam and normal direction of the sample surface. The arc-shaped dark fringe in the image is the lateral profile of the mesa structure. The profiler measure result shows that the height of the mesa structure is 2.4 $\mu\text{m}$ .

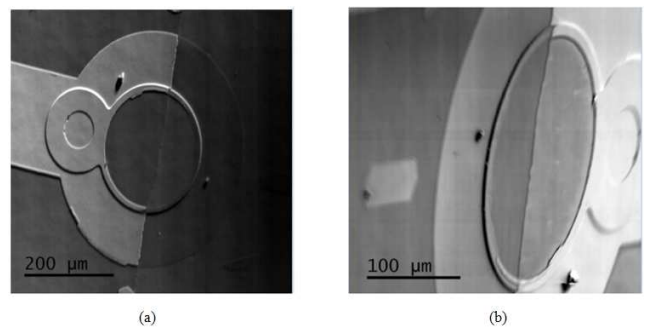


Figure 3. SEM image of the sample (30kV).

(a) Electron beam scanning perpendicular to the sample surface (b) Electron beam is incident at 162° to the normal of the sample surface.

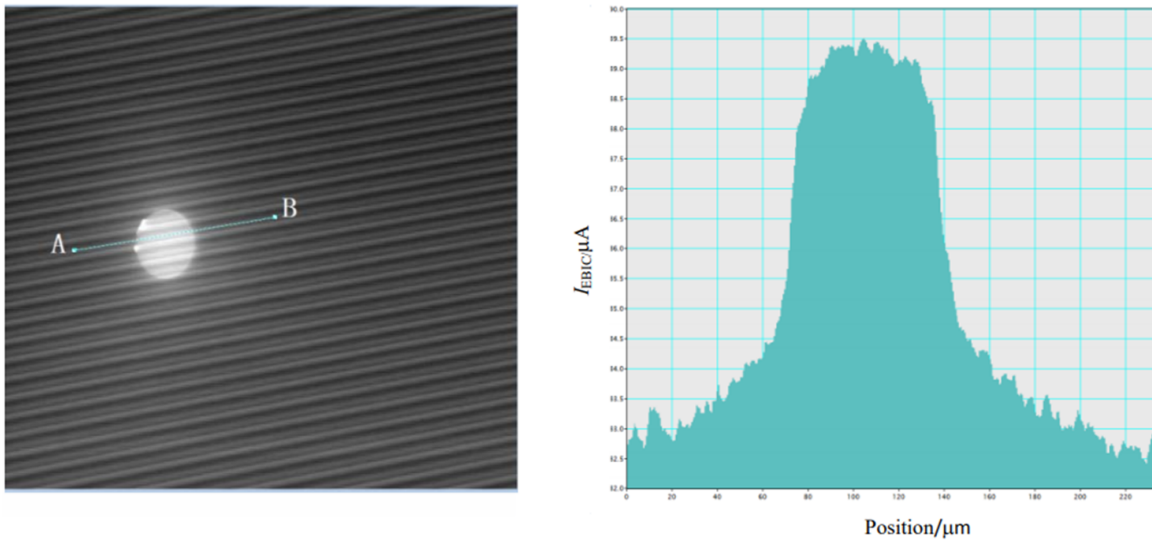
### 3. Junctions in InSb Devices

#### 3.1. Schottky Junction

Schottky junction is a simple interface between metal and semiconductor. It is similar to a p-n junction in their nonlinear impedance characteristics (rectification characteristics). The Schottky junctions formed with different metals and different semiconductors will have different potential barrier height. The height will change when apply an external bias to Schottky junction. When apply positive bias to the metal side of Schottky junction, the potential barrier height will be lower and the charged carrier will easily pass through the barrier. And vice versa. So, the Schottky junction has rectification characteristics (unilateral conductivity). Compared with a p-n junction, the Schottky junction has a distinguishing feature that the current flow through the junction will mainly be formed by majority carriers. Therefore, the Schottky junction

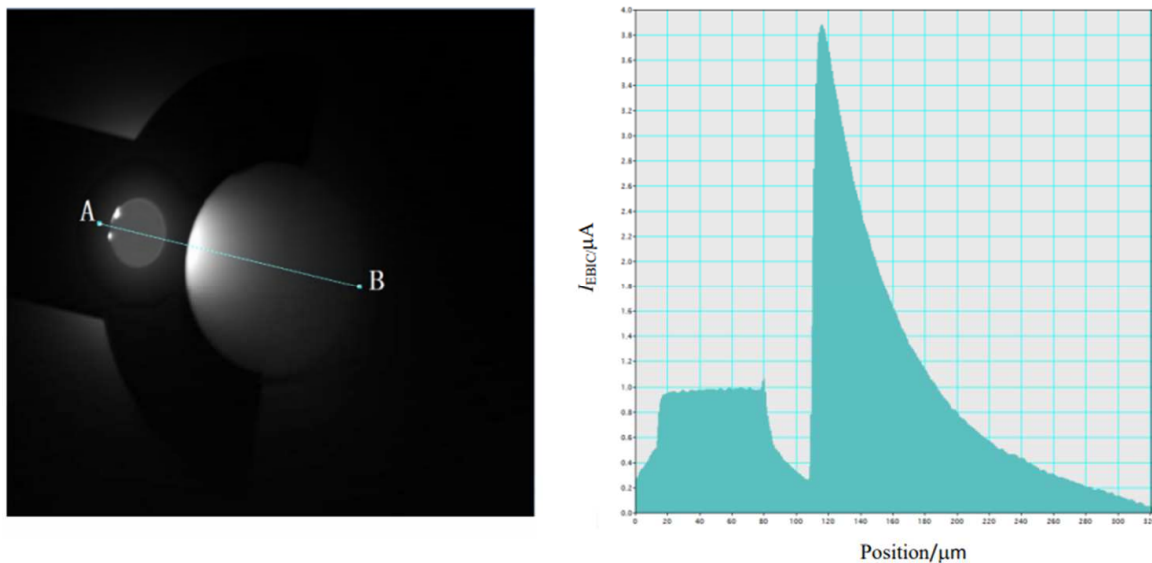
has less charge storage effect and less reverse recovery time.

Figure 4 is an EBIC image which the sample's temperature is 300K and the electron beam's accelerating voltage is 30kV. In the image, most area is dark except the Ohm hole which appears a little light bright. (See Figure 4(a)). The EBIC signal appears at the Ohm hole but it is a small signal. A current distribution between A and B in Figure 4(a) is displayed in Figure 4(b). The graphic shows that the biggest EBIC signal is 0.89 $\mu$ A while the average background noise current is 0.81 $\mu$ A. (The signal and the noise have the microamps level because they have been amplified synchronously. In fact, the real EBIC signal is much smaller than the displayed value, similarly hereinafter). In EBIC measurement, if EBIC signal is small or naught, the screen will display the background noise. When the EBIC signal is far bigger than the background noise, the screen will mainly display the EBIC signal while the background noise will be hidden.

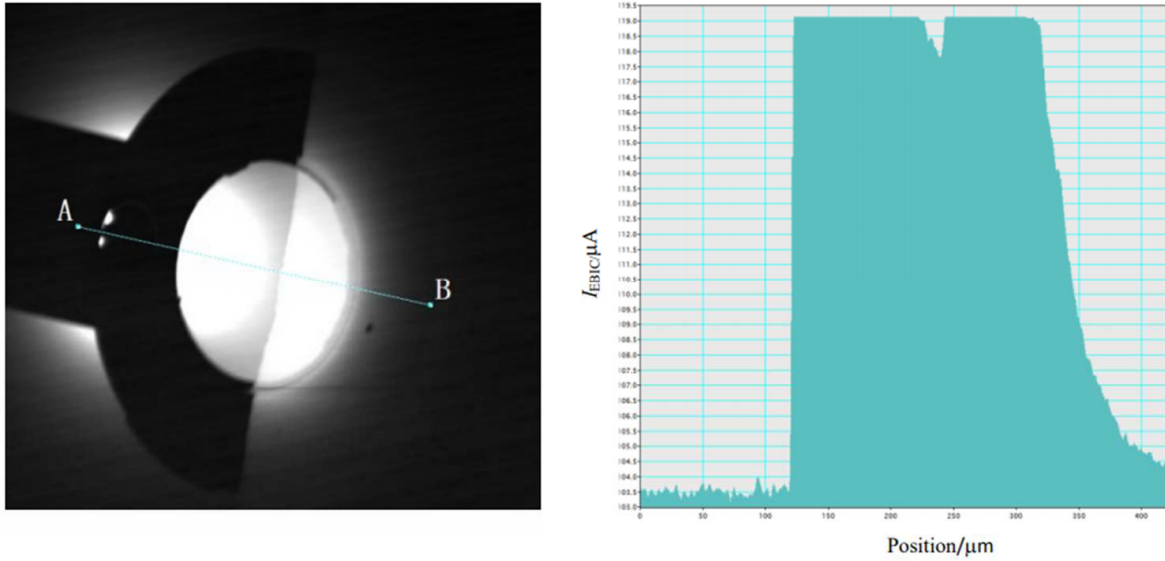


Note: The horizontal axis on the right is position between A and B (similarly hereinafter)

Figure 4. EBIC image of the sample (left) and the profile of EBIC between A and B (right) (30kV, 300K).



(a) External bias: 0V



(b) External bias: 0.001V

**Figure 5.** EBIC image of the sample (left) and the profile of EBIC between A and B (right) (30kV, 80K).

Figure 5 is the sample's EBIC image when the sample's temperature is 80K. The electron beam's accelerating voltage is 30kV. Figure 5(a) is the EBIC image and the EBIC distribution between A and B under the condition of zero external bias. Figure 5(b) is the EBIC image and EBIC distribution between A and B under the condition of 0.001V external bias. Figure 5(a) shows that EBIC signal appears both the Ohm hole area and the mesa structure area (photosensitive area). The intensity of EBIC signal in photosensitive area is obviously bigger than that in Ohm hole and other area. When applies 0.001V positive external bias to the p-n junction, both the intensity and the area of EBIC signal increase remarkably. The area of EBIC signal expands from the Ohm hole to 1/4 of photosensitive area. Compared with Figure 5(a) and Figure 5(b), in Figure 5(a) the biggest EBIC signal is  $4\mu\text{A}$  and the average EBIC signal in Ohm hole area is  $0.9\mu\text{A}$ , in Figure 5(b) the average EBIC signal in Ohm hole area is  $5.4\mu\text{A}$  and the EBIC signal in photosensitive area appears saturation. When remove the 0.001V external bias, the EBIC measurement results quickly return to that in Figure 5(a).

EBIC signal results from the extra removable nonequilibrium carriers (electron hole pairs) which flow through the space charge region. These carriers are produced by electron beam stimulation in junction region. Figure 4 indicates that there is a junction (space charge region) between p region and Cr. When the sample's temperature decreases, the junction will extend out. Figure 5(a), (b) indicate that the expanding junction area has nonlinear impedance characteristics (rectification characteristics). *Therefore, this expanding junction is just Schottky junction!* The expanding Schottky junction is also called Schottky response zone. The size of Schottky response zone formed from different metals and different semiconductors are different. This size can be expressed by the distance between

the margin of the zone and the interface of metal-semiconductor. So far, there is no report on the specific data for different Schottky response zones [10]. From Figure 5(a), it can be measured that the Schottky zone expands to a round area which has its center at the center point of Ohm hole and its radius of  $80\mu\text{m}$ . It can be calculated that under the condition of 80K and 0 external bias, the Schottky response zone is  $47\mu\text{m}$  for a Cr-InSb Schottky junction. It is clear that the Schottky response zone shows distinct temperature dependence: the response zone will expand while its temperature decrease.

### 3.2. p-n Junction

Figure 6 is the EBIC image (left) and the EBIC distribution (right) between A and B under the condition of 80K (sample's temperature), 15kV (electron beam's accelerating voltage), and 0.001V (positive external bias). There are two relatively big bright areas. The EBIC signal in two areas are all saturated. (See the profile in Figure 6 (right)). The first bright area (near the Ohm hole) is the Schottky response zone which is enlarged compared with it in Figure 5(b). A possible explanation is that there exist two junctions in this area. One is the Schottky response zone and another is the p-n junction (a p-n junction was pre-implanted in the mesa structure (photosensitive area)). When electron beam stimulation happens, two junctions will together contribute for the extra removable nonequilibrium carriers (electron hole pairs) production that causes EBIC signal increase and the bright area enlarged. The second bright area (crescent in shape) has a uniform brightness. The EBIC signal has uniform distribution in this area. There are no dark spots in this area. This means there is no defects in this area. The p-n junction in this area is relatively uniform.

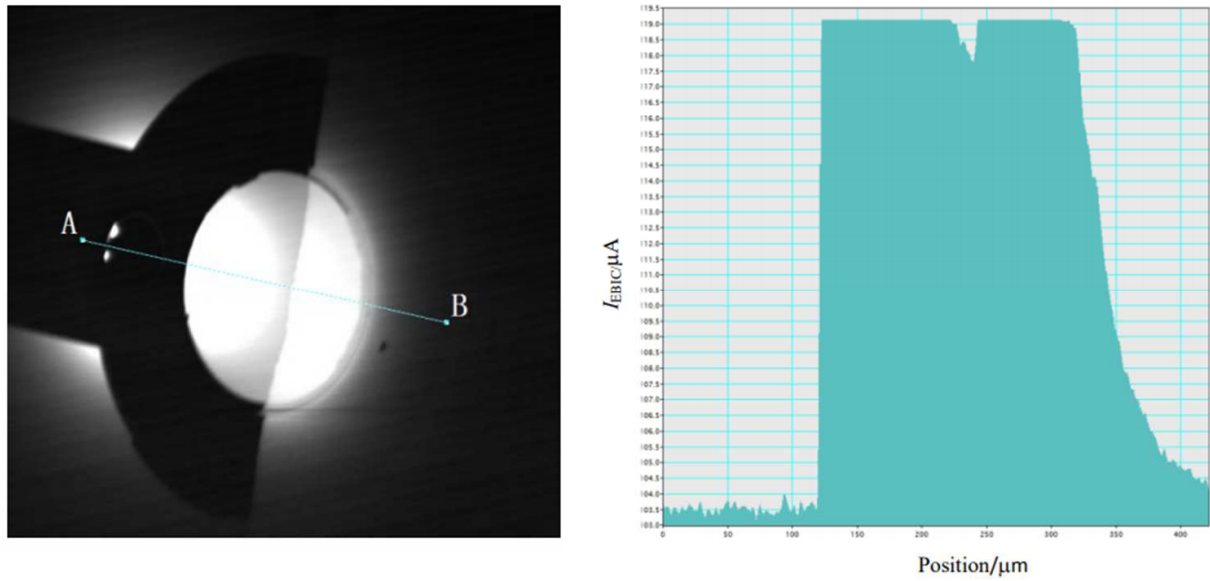


Figure 6. EBIC image of the sample (left) and the profile of EBIC between A and B (right) (15kV, 80K).

Figure 7 is the EBIC image (left) and the EBIC distribution (right) between A and B under the condition of 80K (sample's temperature), 9kV (electron beam's accelerating voltage), and -0.001V (negative external bias). In Figure 7, the Schottky junction response zone shrinks. This zone is almost covered by metal film. This shrinkage indicates that the -0.001V (negative external bias) reduces the space charge region of the Schottky response zone. This feature is consistent with the unilateral conductivity

(rectification characteristics) of Schottky junction. The bright area (crescent in shape) has uniform brightness, clear edge profile and proper contrast. In this area, the EBIC signal distributes uniformly. It indicates that the p-n junction in this area is well structured. It also indicates that proper electron beam's energy, the depth which the p-n junction was implanted from the surface of sample, the passivation film's thickness and materials altogether result good EBIC measurement.

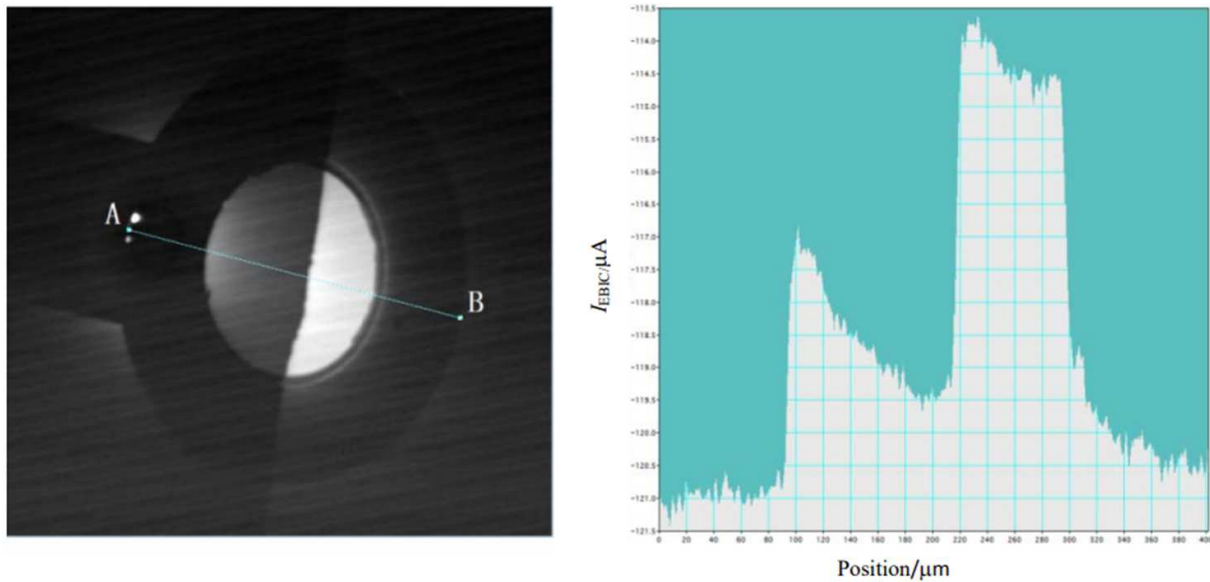
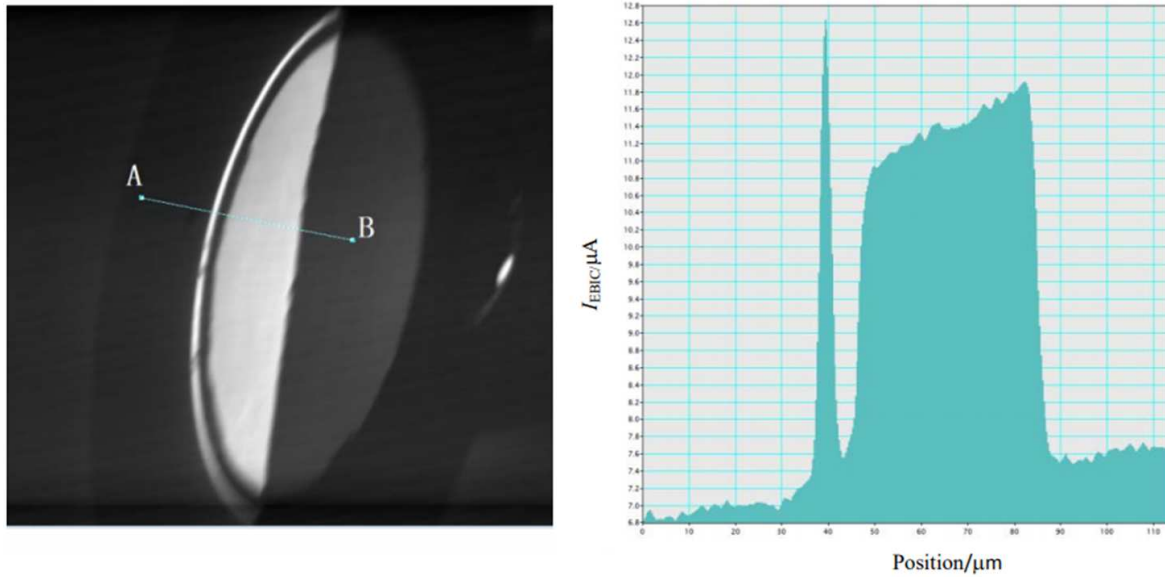


Figure 7. EBIC image of the sample (left) and the profile of EBIC between A and B (right) (9kV, 80K).

Figure 8 is the lateral side's EBIC image (left) and the EBIC signal distribution (right) between A and B of the mesa structure (photosensitive area) under the condition of 80K (sample's temperature), 9kV (electron beam's accelerating voltage), and 0V (external bias). The angle between electron beam and normal direction of the sample surface is 162°. The arc shaped bright stripe is the EBIC

image of p-n junction implanted in the mesa structure. From the EBIC signal distribution, the biggest EBIC signal is 1.3μA. There is an arc shaped dark stripe between the arc shaped bright stripe and the crescent shaped bright area. This is because the passivation film thickness on the arc shaped dark stripe is thicker than that on the crescent shaped bright area.



**Figure 8.** EBIC image of the sample side (left) and the profile of EBIC between A and B (right) (9kV, 80K).

When the electron beam scanning was focused in a small scope, for example: the arc shaped stripe scope, the SEM image of the small scope was amplified. The amplified SEM image is displayed in Figure 9(a) under the condition of amplification times 10000. The dark stripe in Figure 9(a) is just the SEM image of the lateral side of mesa structure. Because of the electron beam scanning and viewing angle, the stripe appears dark. From the measurement, the width  $W$  of the dark stripe is  $W= 2.5\mu m$ . There is an angle of  $162^\circ$  between electron beam and normal direction of the sample surface. Therefore, the practical height  $h$  of the mesa structure can be calculated from the following express:

$$h=W\sin\alpha \tag{1}$$

here  $\alpha=72^\circ$ . So, the practical height  $h$  of the mesa structure is  $2.4\mu m$ , and this is accordant with the result of profiler

measurement. Figure 9(b) is the EBIC image of the area in Figure 9(a). The bright stripe in Figure 9(b) is the position of p-n junction that was implanted in mesa structure. The EBIC signal distribution between A and B in Figure 9(b) is displayed in Figure 10. It appears that EBIC signals' spatial gradient (the slope of EBIC signal distribution's envelope line) in the left part of the image is greater than that in the right part of the image. The left part of the image corresponds to the n region of the sample while the right part of the image corresponds to the p region of the sample. The EBIC signal's spatial gradient can reflect the structure of the space charge region. Therefore, it indicates that there is a thinner space charge region with greater density of space charge on the side of n region, and there is a thicker space charge region with smaller density of space charge on the side of p region (the position of biggest EBIC signal as the dividing line between n region and p region).

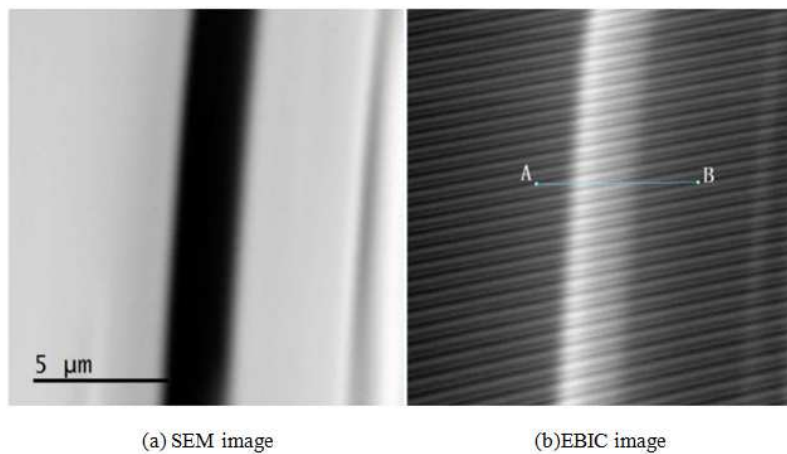


**Figure 9.** SEM and EBIC Image of the sample (8kV, 80K).

The p-n junction was formed by injecting  $Be^+$  ions into the sample. Though these ions have constant energy and stable ion beam, when these ions strike into the sample, they will

take interaction with atoms or ions of passivation material ( $SiO_2$ ) and substrate material (InSb) and lose some energy. Most of  $Be^+$  ions will reach to a certain depth (e. g. the

position of the biggest signal in Figure 10) of the sample surface and will be mounted there. A small part of  $\text{Be}^+$  ions, which strike many times with material's atoms or ions, lose more energy and reach to a shallow depth. These  $\text{Be}^+$  ions,

even though they have small quantity and “fall behind”, have contribution to the space charge region and density of space charge. They cause the thicker space charge region and smaller density of space charge on the side of p region.

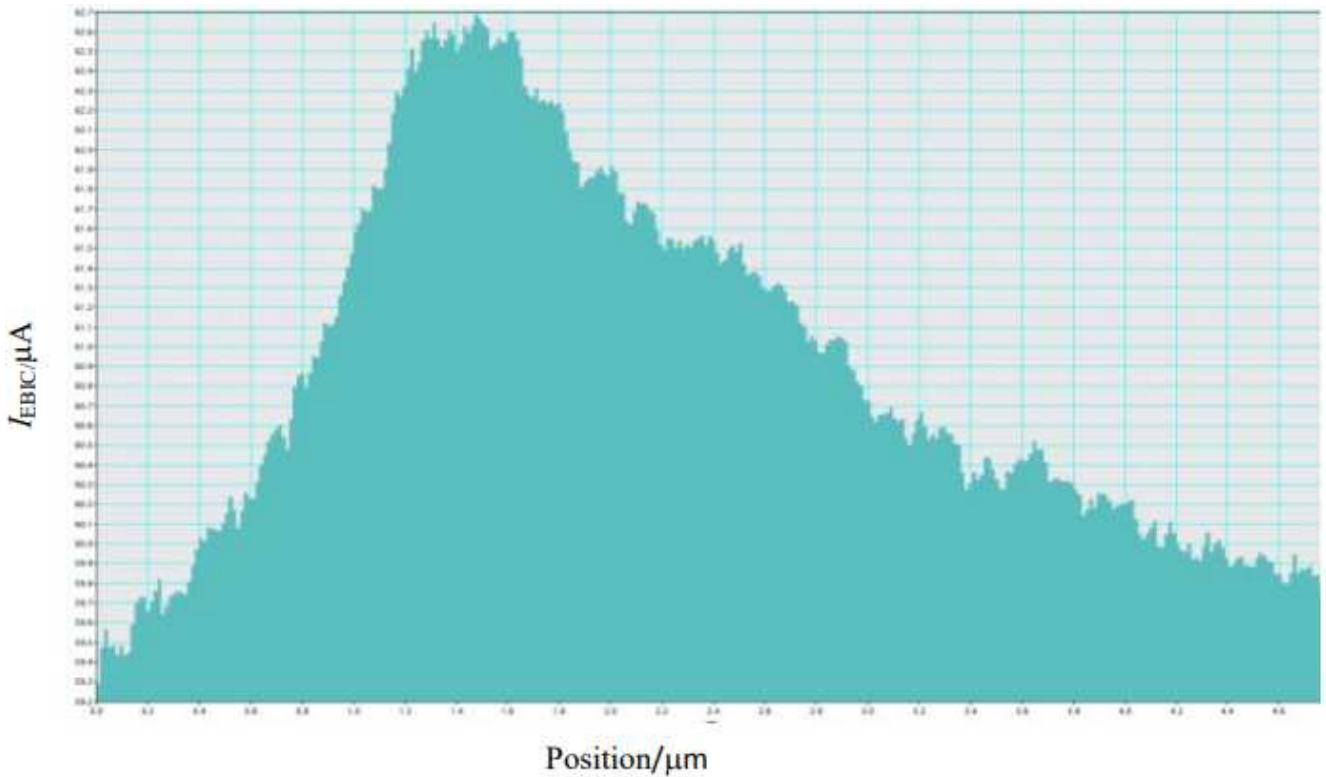


Figure 10. Profile of EBIC between A and B in Figure 9(b).

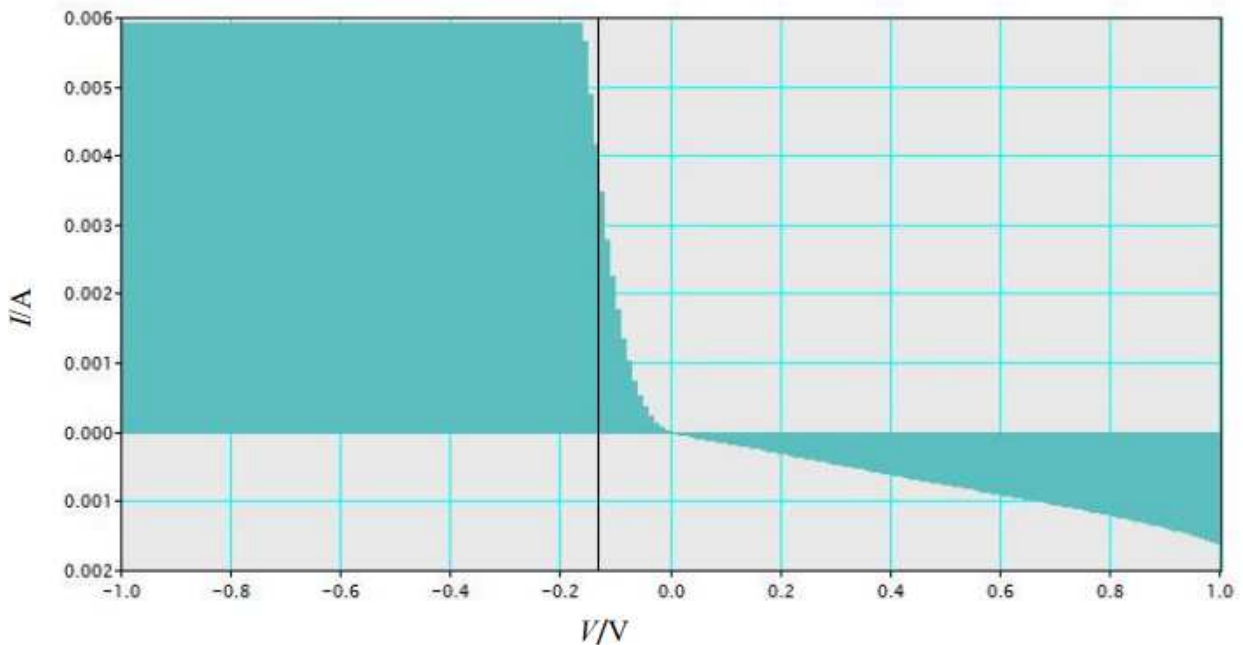


Figure 11. *I-V* characteristics of the sample (80K).

Figure 11 is sample's *I-V* characteristics under the condition of 80K (sample's temperature), <1Pa (vacuum of SEM chamber). The *I-V* characteristics indicates that the

sample has typical characteristics of a diode. Because a small part of passivation film was etched off, the passivation film does not protect the InSb device very well. This causes the

reverse characteristics of the diode less perfect.

## 4. Conclusion

Initially, EBIC was employed to observe the width and the position of the sample's p-n junction. When executed the observation, the temperature dependence of Cr-InSb Schottky junction was discovered unexpectedly. When Schottky junction's temperature decrease, Schottky junction itself will have a new space charge region. This new space charge region is out of Schottky junction itself. Both the new space charge region and Schottky junction's space charge region have same character. The new space charge region will enlarge with temperature decrease. This new space charge region is called Schottky response zone. Experimental result demonstrates that with temperature decrease, Schottky junction's potential barrier will lower. The electron hole pairs caused by electron beam stimulation increase and EBIC signal increase. The p-n junction fabricated using ion-beam implantation in the InSb device has an asymmetrical spatial distribution. The aforementioned region on the n-type side is thinner and has larger charge density than that on the p-type side. This is an inherent characteristics of junction formation by ion implantation. How to eliminate or to effectively use this case is the task of further study. As one of the most useful analytical methods, EBIC offers the advantage of a microscopic and perspective view for the observation and analysis of semiconductor devices. With proper measurement condition, the devices' (such as Schottky junction, p-n junction etc.) depth and positions can be measured or observed without damaging the devices themselves. From Figure 8 and Figure 9, EBIC can measure the devices to the micrometer in geometry dimension.

---

## References

- [1] YANG Deren. A Test and Analysis on Semiconductor Materials [M]. Beijing: Science Press, 2010.
- [2] CHEN Boliang, ZHANG Yueqing, FANG Xiaoming, et al. Determination of hole diffusion length in n-InSb at 80K [J/OL]. Proceedings of SPIE, 2001, 4369: <https://doi.org/10.1117/12.445309>.
- [3] FAN Dingxun, Neelu Kang, Sepideh Gorji Ghalamestani. Schottky barrier and contact resistance of InSb nanowire field-effect transistors [J]. Nanotechnology, 2016, 27: 275204.
- [4] Hardingham C. A novel, non-destructive, technique using EBIC to determine diffusion length in GaAs solar cells [C]/Proc. of 25thPVSC, 1996: 231-234.
- [5] Higuchi H, Tamura H. Measurement of the lifetime of minority carriers in semiconductors with a scanning electron microscope [J]. Japanese Journal of Applied Physics, 1965 (4): 316-317.
- [6] Berz F, Kuiken H K. Theory of life time measurements with the scanning electron microscope: steady state [J]. Solid-state Electronics, 1976, 19: 437-445.
- [7] Donolato C, Kittler M. Depth profiling of the minority-carrier diffusion length in intrinsically gettered silicon by electron-beam-induced current [J]. Journal of Applied Physics, 1988, 63 (5): 1569-1579.
- [8] Cathodo luminescence at p-n junction in GaAs [J]. Journal of Applied Physics, 1965, 36 (4): 1387-1389.
- [9] Miyazaki E, Miyaji K. Enhancement of reverse current in semiconductor diodes by electron bombardment [J]. Japanese Journal of Applied Physics, 1965 (2): 129-130.
- [10] Dereniak E L, Boreman G D. Infrared Detectors and Systems [M]. Wiley Interscience Publication, 1996: 439-452.